

Pion charge exchange to the isovector giant dipole state at energies above the 3-3 resonance

R. A. Loveman,* B. L. Clausen,[†] and R. J. Peterson

Nuclear Physics Laboratory, University of Colorado, Boulder, Colorado 80309

S. H. Rokni[‡]

Utah State University, Logan, Utah 84322

H. W. Baer, A. G. Bergmann,[§] J. D. Bowman, F. Irom, and C. J. Seftor[§]

Los Alamos National Laboratory, Los Alamos, New Mexico 87545

J. Alster and E. Piasetzky

Raymond and Beverly Sackler Faculty of Exact Science, Tel Aviv University, Tel Aviv, Israel

J. N. Knudson

Arizona State University, Tempe, Arizona 85287

U. Sennhauser

Paul Scherrer Institute, CH-5232 Villigen, Switzerland

(Received 31 July 1989)

Small-angle differential cross sections for the (π^+ , π^0) reaction have been measured at energies of 300, 425, and 500 MeV for the isovector giant dipole resonance in a range of targets. Peak differential cross sections are inferred by extrapolation in angle. The target-mass dependence of these cross sections, normalized to the expected sum rule, shows the same mass dependence at 425 MeV that is observed for isobaric analog state transitions.

I. INTRODUCTION

Isovector giant resonances are well established nuclear normal modes of great current theoretical interest¹⁻⁴ and well known from charge-exchange experiments using pion meson beams.⁵⁻⁹ Charge exchange, either with pions or nucleons, is a specific probe of these states as it can excite only isovector modes, and measurements of cross sections for single charge exchange with pions and nucleons complement each other, as pions excite primarily electric modes (no spin flip) and nucleons at intermediate energies excite primarily magnetic modes (spin flip).

The energy dependence of the pion-nucleon interaction may also be exploited to gain information about the transition densities for isovector giant resonances. At the peak of the $\Delta(1232)$ resonance, the classical mean free path for pions in nuclear matter is about 0.7 fm. At $T_\pi = 500$ MeV, this has increased to 2.5 fm. Consequently, it is expected that such a variation of the pion energy will allow a probing of different depths of the nucleus and hence of the transition density.

We report here measurements of the maximum differential cross section for pion single charge exchange (SCX) to the giant dipole resonance (GDR) at beam energies of 300, 425, and 500 MeV. In this energy range we find that differences in cross sections for different nuclei are much more pronounced than at energies near the Δ resonance,⁵⁻⁹ and that there is a dramatic increase in the cross section between 425 and 500 MeV. The data we present are for five nuclei, ²⁷Al, ⁶⁰Ni, ⁹⁰Zr, ¹²⁰Sn, and

²⁰⁸Pb at an incident pion energy of 425 MeV, and a study of the energy dependence of the cross section for the GDR for ⁶⁰Ni and ²⁷Al.

The present GDR measurements complement studies of pion charge exchange to the isobaric analog state (IAS) over a wide range of energies.¹⁰⁻¹⁵ Near the Δ resonance these results have shown that the interaction between the pion and the nucleus cannot be simply dealt with using first-order optical potentials or other first-order methods. However, the recent measurements for the IAS at higher energies have shown that the pion nucleus interaction simplifies at energies above the $\Delta(1232)$ resonance.¹⁵

Near the Δ resonance, pion charge exchange to the isovector GDR and monopole (GMR) peaks has determined the excitations and widths for these normal modes and has shown that the transitions exhaust large parts of the calculated sum-rule strength.^{5,8,9} Maximum differential cross sections are almost the same for all target nuclei,⁸ whereas the IAS cross sections vary greatly in strength,^{11,14,15} depending upon ($N-Z$) as well as distortions. A few measurements for exciting the giant isovector resonances have also been made at energies slightly above and below the Δ resonance.⁹ Once again these measurements show little variation of the maximum differential cross sections among different nuclei, but they do show a rise in this cross section with increasing beam energy.

Measurements of the cross sections for exciting the isovector monopole resonance (IVMR) have been reported in several papers.⁶⁻⁹ The measurements we report here

have neither the angular range nor the statistical accuracy necessary to determine whether the IVMR is excited. Therefore, though fits were made to what might be the IVMR, this was considered to be a background for our analysis of the GDR.

Giant dipole states built upon isobaric analog states are observed in pion double charge exchange,¹⁶ with cross sections determined in a two-step mechanism by both IAS and GDR SCX cross sections. Pion DCX reactions have been measured from 300 to 500 MeV,¹⁷ with recent experiments examining the GDR peaks as well. The present SCX data to the GDR, together with high-energy measurements to the IAS,¹⁵ provide the information necessary for a sequential model of the DCX data.

II. EXPERIMENTAL DESIGN AND ANALYSIS

The experiment was performed with the π^0 spectrometer¹⁸ at the P^3 channel at the Clinton P. Anderson Meson Physics Facility. The π^0 spectrometer consists of a pair of position-sensitive gamma calorimeters which were set up on two separate posts. The opening angles between the two calorimeters were 36.15° at 300 MeV, 28.15° at 425 MeV, and 24.56° at 500 MeV. These posts were set so that there was a distance of 2.02 meters between the target and the first gamma converter of each calorimeter, symmetric about zero degrees.

The effective solid-angle normalization of the π^0 spectrometer at each energy was obtained by using CH_2 targets, measuring the $\pi^- p \rightarrow \pi^0 n$ reaction at each energy.¹⁹ The energy resolution was 5.4 MeV FWHM at 300 MeV and 12.8 MeV FWHM at 500 MeV. This was nearly equally due to the intrinsic resolution of the π^0 spectrometer and beam-associated effects.

The incoming π^+ flux was determined by the ^{11}C activation technique.²⁰ At these high pion energies there is a significant proton contamination to the pion beam, even after use of an absorber system, and since protons in the pion beam can also induce ^{11}C activity, the ratios of protons to pions in the beam had to be measured. This was done using a sampling grid scintillator based on the design of Ref. 21. The proton-to-pion ratio was found to vary from less than 0.01 at 300 MeV to 0.29 at 500 MeV. With corrections for the proton contamination the pion flux was determined to vary between $1 \times 10^7 \pi^+/\text{s}$ at 300 MeV to $2.5 \times 10^6 \pi^+/\text{s}$ at 500 MeV. Target thicknesses ranged from 0.84 g/cm² for ^{27}Al to 2.24 g/cm² for ^{208}Pb .

Extracting giant resonance cross sections from the differential cross sections measured is limited in accuracy primarily by the ability to separate scattering to the giant resonance in question from the background. This background may include other giant resonances, continuum nuclear states, and quasifree scattering. The data we present show a background and very clear peaks from excitation of the IAS (which has been previously analyzed¹⁵) and the GDR (see for example Fig. 1). For the analysis of these data, the background is distinguished from the GDR and IAS peaks by both peak shape and angular dependence. This method is identical to that used in several previous studies of GDR excitation by pion SCX.^{8,9}

Data were sorted into three angular bins during analysis to determine a partial angular distribution. The mean scattering angles including the detector acceptance for the bins were approximately 2, 4, and 6 degrees. These varied slightly for different energy-target combinations.

A phenomenological model for the background incorporating the basic features one expects from quasifree scattering has been previously used for projectile pion energies near the Δ resonance^{8,9} and is again used here.

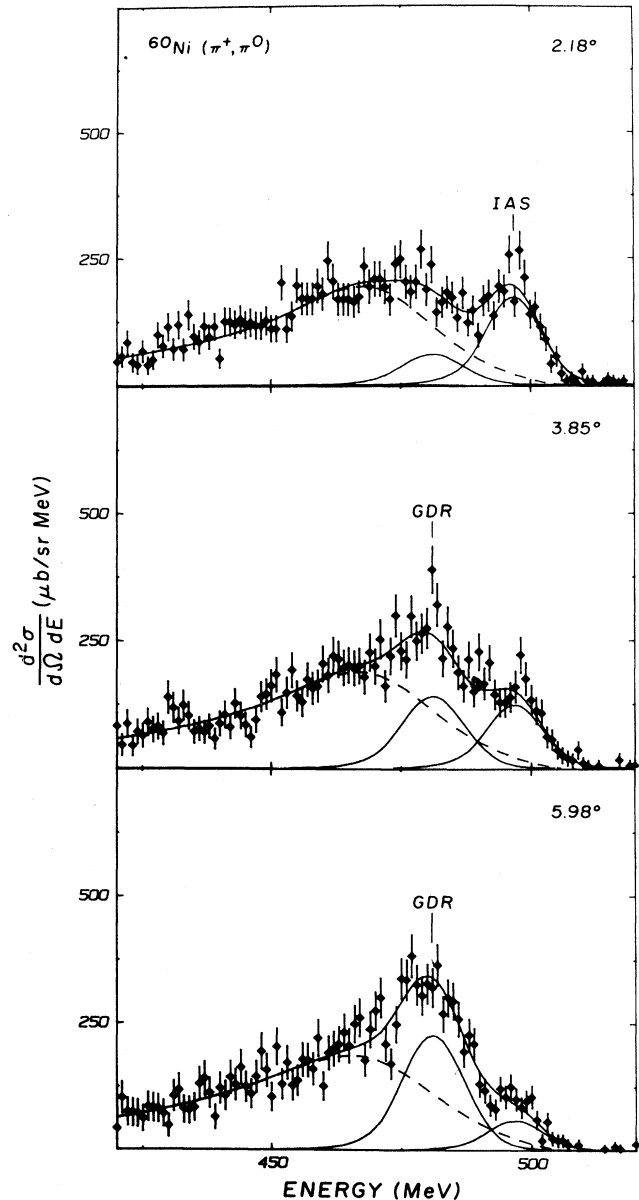


FIG. 1. Spectra for the $^{60}\text{Ni}(\pi^+, \pi^0)$ reaction are shown for a beam energy of 500 MeV for three angular bins. The central angle for each bin is indicated. The curves show the fits described in the text, with the IAS peak at highest pion beam energy, the GDR peak treated in the present work and a dotted curve for the background. At larger angles the GDR peak area increases.

The specific formulae used to characterize the background are found in Ref. 7; these previous studies had the advantage of a considerably larger angular range than we have measured. The pion momenta are larger for the present measurements than for previous measurements, and this in part compensates for our small angular range by shifting the spectra to smaller angles. Measurements of SCX excitation of the GDR in several nuclei have shown that they have widths ranging from 3 MeV to 10 MeV.^{8,9} This is narrow compared to the effective widths of the backgrounds which are typically ~ 23 MeV.^{8,9} In contrast, the measured widths for IVMR states are typically about 18 MeV,^{6,8,9} roughly the same as the backgrounds.

Even with a narrow peak such as the GDR, several of the background parameters, which in previous studies were allowed to vary, in this study had to be held fixed. In particular, these data were not sufficient to allow a good determination of any of the parameters relevant to the angular dependence of the background. For these fits, the background angular dependence was assumed to be only second order in q/k_f where $q = 2k \sin(\theta/2)$ and k_f is the Fermi momentum. Terms in the background angular dependence that were fourth order in q/k_f were set to zero. The coefficient for the second-order term, A_1 , was fixed at 3.40 for all nuclei. This value is roughly an average value for A_1 from the data of Erell *et al.*,⁸ which were taken at 165 MeV. Coefficients for the first-order term are listed as A_0 in Table I.

In addition to the normal background used in previous

studies, the IVMR was treated as a part of the background, but concentrated in excitation energy and scattering angle. Only the strength of the IVMR was allowed to vary freely while its width and the difference between the IVMR excitation energy and the GDR excitation energy were fixed. Values used for these were either taken directly from the data of Erell *et al.*⁸ or, where those values had not been measured for (π^+, π^0) scattering, were extrapolated assuming they were a smooth function of A . Generally, the A dependences of these particular quantities were quite weak, and errors due to this extrapolation are small. Uncertainties in the cross sections due to background uncertainties are discussed in the following.

Table I shows the background parameters, using the terminology of Ref. 8. As can be seen in this table, the energy and A dependences for these parameters are smoothly varying. The IVMR cross sections were only to be regarded as a representation of part of the background and are not listed.

The GDR peaks were fit by folding a Gaussian resonance shape with the peak shape measured from the $\pi^- p \rightarrow \pi^0 n$ reaction. In order to extract cross sections consistent with previous studies, the widths of the GDR's were fixed to the values found by Erell *et al.*⁸ for (π^+, π^0) scattering. While the widths of the GDR's were fixed, the positions were allowed to vary. This allowed us to check to see if we were examining the same excitation as had been previously studied. By taking the difference between the central energies of the IAS and the GDR exci-

TABLE I. Parameters used for fitting the charge exchange spectra to extract GDR cross sections are listed, using the form given in Refs. 8 and 9. W_{Lo} is the width of the Lorentzian shape for quasifree scattering, with CB an adjustment due to the Coulomb energy from the true quasifree (QF) energy required by the data. The energy interval for the fitting is determined by E_0 and T . An IVMR peak of known excitation and width was included in the fit, with the 0° strength varied to fit our data. This is not a valid analysis of the IVMR strength, and no strengths are listed. The ground state of the daughter nucleus is at the expected energy labelled GS . We use the radius R for the Bessel function fits. Our background is then given by the IVMR and

$$d^2\sigma/d\Omega dE = N\{1 - \exp[(E - E_0)/T]\} / \{1 + [(E - E_{QF})/W_L]^2\}$$

with

$$E_{QF} = T(\text{free}) - CB - \text{proton binding energy}$$

and $W_L = W_{Lo}(1 + \alpha q^2/k_f^2)$, with α , CB , and T from Ref. 8.

Target	A_0	W_{Lo} (MeV)	CB (MeV)	E_0 (MeV)	T (MeV)	GS (MeV)	R (fm)
300 MeV							
²⁷ Al	0.08	26.7	4.80	261.1	70	335.7	4.30
⁶⁰ Ni	0.60	31.6	7.92	285.0	70	300.4	4.94
425 MeV							
²⁷ Al	0.42	37.3	4.80	416.1	70	424.9	4.24
⁶⁰ Ni	0.93	30.8	7.92	411.6	70	431.0	5.46
⁹⁰ Zr	0.74	23.4	9.89	406.5	70	430.6	5.67
¹²⁰ Sn	1.13	22.4	11.23	415.6	70	429.3	6.67
²⁰⁸ Pb	1.50	22.1	15.33	417.6	70	425.9	8.29
500 MeV							
²⁷ Al	0.58	22.3	4.80	499.7	70	494.4	4.26
⁶⁰ Ni	0.61	26.9	7.92	477.8	70	505.7	4.56

tations, values for the excitation in the final nucleus were derived. These values were in agreement with the values measured by Erell *et al.*⁸ and Irom *et al.*,⁹ who measured cross sections for SCX excitation of giant resonances at lower beam energies for all of the targets in this study except ²⁷Al. For this nucleus the width and excitation energy of the GDR were fit separately for each energy. The results at the three energies measured agree with each other within statistical errors.

The differential cross section for excitation of the GDR was assumed to have a $J_1^2(qR)$ angular dependence. A single radius R was determined for each energy-nucleus combination by simultaneously fitting the data for both the GDR and the IAS at all three angles to $J_1^2(qR)$ and $J_0^2(qR)$, respectively. Extrapolations from the peak cross sections measured for the GDR to the maximum differential cross section were made using the $J_1^2(qR)$ angular dependence with the fit radius and these maxima were typically near 25 percent above the largest measured cross section. Values for R are listed in Table I. As a check of our fitting procedure, we also extrapolated the IAS cross section to zero degrees using a $J_0^2(qR)$ angular dependence and compared these values with published values.¹⁵ Agreement was found in all cases to within two standard deviations, and to differ by more than one standard deviation in only three out of nine cases.

Errors from the fitting procedure were broken up into three major types. These were errors due to the statistical accuracy of the data, errors due to assumptions made about the nature of the background, and errors due to the extrapolation from the measured differential cross sections to the maximum differential cross section. Each of these was assumed to be independent of the other two and they were therefore added in quadrature to obtain the total uncertainty, from the fits to the data.

The fits to the data produced the error matrix and the error in the variable as part of the fitting procedure. This is the error due to the statistical accuracy of the data.

Fits were made to the data assuming three different angular dependences to the background in order to analyze errors this might produce in the differential cross sections. First, the coefficient A_1 for the second-order term in q/k_f was changed from 3.40 to zero. This eliminates the angular dependence to the background and is equivalent to a subtraction of the data from the large-angle and small-angle bins. Second, this coefficient was changed to 5.00. This enhanced the angular dependence of the background significantly. Finally, the strength of the IVMR was set to zero, and the coefficient for the second-order term in q/k_f was allowed to fit the data freely. It was necessary to fix the strength of the IVMR to some value in order to make this fit to the value of the A_1 coefficient because there was an extremely strong correlation between its value and the strength of the IVMR. This correlation was a direct reflection of the limited angular range of these data.

The maximum differential cross section was determined separately for each of these conditions and the differences between each of these three and the cross section from the standard fit described earlier were determined. The largest of these three differences for each

target-energy combination was taken to be the contribution to the error by the fitting assumptions.

An angular dependence for the differential cross section was assumed in order to extract peaks from the data. Previous studies had used shapes determined by DWIA calculations,^{8,9} but these calculations cannot include d -wave pion-nucleon scattering amplitudes, necessary at our high energies. Previous studies had also found that the differential cross sections for the giant resonances were well described by diffractive scattering.

For analysis of these data, the angular dependence of the differential cross section was assumed to be diffractive with a standard $J_L^2(qR)$ shape for an excitation with angular momentum $L\hbar$.²² The dominant features of the data were the background which had only a small angular dependence, the IAS and the GDR, both of which have strong angular dependences. Consequently, the strong absorption radius was determined primarily by the dropoff of the IAS and the increase in the GDR differential cross sections as the angle was increased. Studies have shown that the strong-absorption radius is well described by a $R = r_0 A^{1/3}$ mass dependence.²² For the mass survey at 425 MeV we determined the data to be consistent with this description with $r_0 = 1.37 \pm 0.05$ fm. The values for R from the data at 300 MeV were also consistent with total reaction cross sections determined at 315 MeV.²³

The strong absorption radius r_0 found for the IAS transition alone was 1.17 fm at 425 MeV.¹⁵ In order to examine uncertainty due to this difference, we fixed the radii for the GDR and IAS to be 1.17 fm at 425 MeV and repeated the analysis. The maximum differential cross section for excitation of the GDR was then determined by fitting the data with this constraint. The difference between this value and the standard value was taken to be the contribution to the error by the extrapolation.

There were several additional uncertainties in the GDR cross sections which were unrelated to fitting the data. Among these were the uncertainty in the target thicknesses, the uncertainty in the π^+ flux, and the uncertainty in the solid angle presented by the π^0 spectrometer. These errors were treated for each target-beam combination, and were added in quadrature with the fitting error to form the total error. The total error was dominated by the fitting errors for all target-energy combinations. The fits to the ⁶⁰Ni spectra are shown in Fig. 1.

III. RESULTS

Extrapolated values for the maximum differential cross section for the GDR from the evaluation of the data are shown in Table II. Additional values from previous studies at other energies are also shown for comparison. An example of an extrapolation is shown in Fig. 2. The diamonds represent the angles at which the data were taken, located at the best single fit of the differential cross section to the data (double differential cross section) at these angles. The hatched region includes the possible fits to these data as determined by the error analysis.

TABLE II. Peak differential cross sections for the (π^+, π^0) reaction to the IVGDR are listed, using the measured or previously known excitation energies and widths.

Nucleus	Excitation energy (MeV)	Width (MeV)	Peak cross section ($\mu\text{b}/\text{sr}$)				
			165 MeV ^a	230 MeV ^b	300 MeV	425 MeV	500 MeV
²⁷ Al	24.1 \pm 3 ^c	6.2 \pm 0.09 ^c			1010 \pm 520	1260 \pm 390	2140 \pm 610
⁶⁰ Ni	24.2 \pm 2 ^c	6.4 ^d	790 \pm 190	1240 \pm 130	970 \pm 160	1690 \pm 267	4040 \pm 750
⁹⁰ Zr	25.4 \pm 5	6.0 ^d	910 \pm 270			2102 \pm 370	
¹²⁰ Sn	23.8 \pm 4	3.4 ^d	860 \pm 340	1820 \pm 230		2040 \pm 580	
²⁰⁸ Pb	26.6 \pm 5	6.0 ^d	840 \pm 450			3820 \pm 840	

^aCross sections from Ref. 8.

^bCross sections from Ref. 9, from Fig. 5, analyzed with a fixed width as in this present work.

^cAverage values from measurements at 300, 425, and 500 MeV.

^dWidth fixed to value from Ref. 8.

A simple mass dependence has been used successfully for the IAS to determine the effects of distortion on the pion flux.^{11,14,15} These analyses use the general form²⁴

$$\frac{1}{|M|^2} \frac{d\sigma}{d\Omega}(\text{max}) = g(E) A^{-\alpha},$$

where for the IAS the value of $|M|^2$ is $(N-Z)$. A similar analysis can be done for SCX excitation of the GDR by using sum rules to determine $|M|^2$. One expects that the effects of distortion should be very similar for the IAS and GDR because both have similar excitation energies, and their transition densities are very similar in shape. In order to determine the transition strength and make this analysis of the GDR, one must make two assumptions.

First, one must assume that the resonances seen in all of the different nuclei exhaust the same portion of the energy-weighted sum rule, taken here to be 100%. Previous studies done in the energy region near the Δ reso-

nance have shown that these resonances exhaust a very large percentage of the sum rule.⁵⁻⁹ This sum rule for $|M|^2$ is defined in Ref. 3.

We cannot use our data to determine the magnitudes of the matrix elements $|M|^2$ without an absolute reaction model, which is not yet developed for the high energies of this work. Instead, we use theoretical values of $|M|^2$ to isolate the target dependence and energy dependence of our data.

One must compute the energy-weighted sum rule for the GDR transition. Techniques vary from relatively straightforward analysis of densities³ to simple analytic expressions for sum rules based on binding energy equations⁴ to RPA calculations.³ All of these result in sum-rule strengths in remarkable agreement with each other. For simplicity and uniformity we have chosen to compute the sum-rule strengths from proton densities based on electron scattering data and we assume that neutron densities are identical. We have compared this result with computed sum-rule strengths using Hartree-Fock nucleon densities and have found that differences in neutron and proton distributions from proton distributions determined by electron scattering data lead to differences of at most a few percent in the sum-rule strengths (see Ref. 3 for procedure and Table III for these comparisons). For the energy of the dipole created with the τ_+ operator, we use the simple relationship that the sum of excitation energies for the GDR states created by the τ_- and τ_+ operators is equal to twice the excitation energy for the dipole state created by the τ_0 operator. Where the state created by the τ_+ operator has been measured, this has been found to be accurate.⁸ For heavy nuclei, e.g., ²⁰⁸Pb, this state has not been found, so there is no way of knowing if the excitation energy determined by this relationship is correct. However, the transition strength to this state is very weak, and its contribution to the sum-rule strength is very small compared to the total sum-rule strength. Consequently, the effect of an incorrect value for the excitation energy for the dipole created by the τ_+ operator is negligible. In Table III we list the sum-rule strengths we use, and in addition the sum-rule strengths computed by various other authors and methods.

The GDR data themselves have large errors and conse-

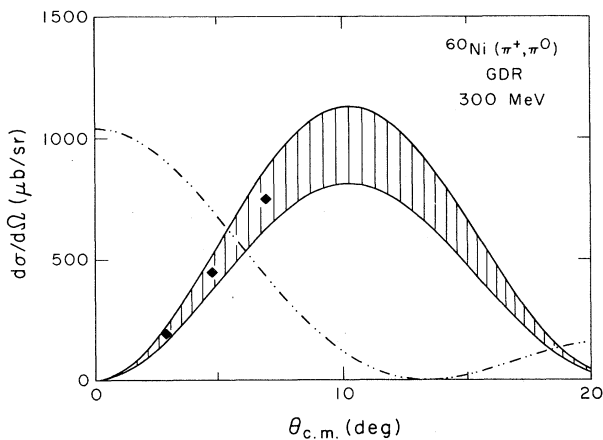


FIG. 2. The measured angular distribution for the GDR peak for ⁶⁰Ni at 300 MeV is shown. The dot-dashed curve shows the $J_0^2(qR)$ shape appropriate to the IAS transition, and the band shows the $J_1^2(qR)$ shape for the GDR transition, using the range of radii R that yield a fit to the three data points. This shape yields the extrapolation to a peak GDR differential cross section of $970 \pm 160 \mu\text{b}/\text{sr}$.

TABLE III. Matrix elements $|M|^2$ in fm^2 as defined in Ref. 3 are listed for (π^+, π^0) charge exchange to the IVGDR for the targets of this study. Several theoretical methods have been used. Cross sections measured in this work are divided by the values in the first column for presentation in Fig. 3.

Nucleus	This study ^a	Ref. 3 ^b	Ref. 3 ^c	Ref. 4 ^d	Ref. 1 ^e
²⁷ Al	9.0				
⁶⁰ Ni	27.8		23.6	17.0	
⁹⁰ Zr	54.9	52.7	44.8	36.7	58.0
¹²⁰ Sn	100.1	99.1	84.2	70.7	
¹⁴⁰ Ce	125.2	105.1			
²⁰⁸ Pb	259.6	251.9	204.0	200.0	

^aFrom sum rules and densities determined by electron scattering.

^bFrom sum rules and densities determined by Hartree-Fock calculations.

^cFrom RPA Hartree-Fock calculations.

^dFrom hydrodynamic model calculations.

^eFrom TDA calculations.

quently do not constrain very much the values of α and $g(E)$ determined by a simultaneous fit. Therefore, in order to compare the distortions for the IAS with those for the GDR, we have made best fits to the GDR data using values for α determined by IAS data at each beam energy while letting $g(E)$ vary to fit the data. We find that the fits with the same exponents on A for the IAS and GDR are quite good (Fig. 3). The χ^2/N_f for 165 and 425 MeV are 0.47 and 0.80, respectively. Additionally, we find that the ratios of the g 's for the two different energies are the same for both the IAS and the GDR. For the IAS, we

find this ratio, $g(165 \text{ MeV})/g(425 \text{ MeV})$, to be 2.55 ± 0.60 , and for the GDR we find this ratio to be 2.59 ± 0.47 .

The energy dependence of excitation of the GDR by SCX is another effective means to examine the pion-nucleus interaction. Figure 4 shows the energy dependence of the cross section for this process on ⁶⁰Ni. The dominant feature is the dramatic increase in the cross section between 425 and 500 MeV. This increase could be due to an increase in the transparency of nuclear

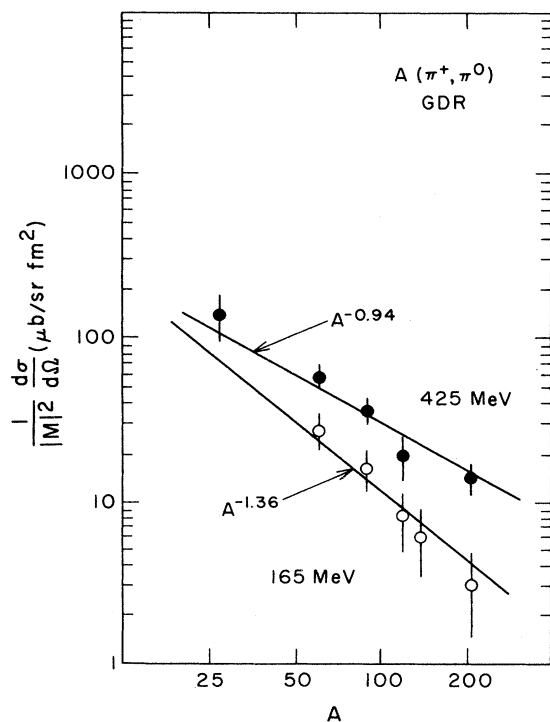


FIG. 3. Peak differential cross sections for pion charge exchange to the GDR are compared to a range of target masses, plotted on a logarithmic scale. These cross sections have been divided by the sum rule strengths $|M|^2$ listed in Table III to remove the most obvious effect of the target mass. These data are fit to the A^α form used also for IAS pion charge exchange.

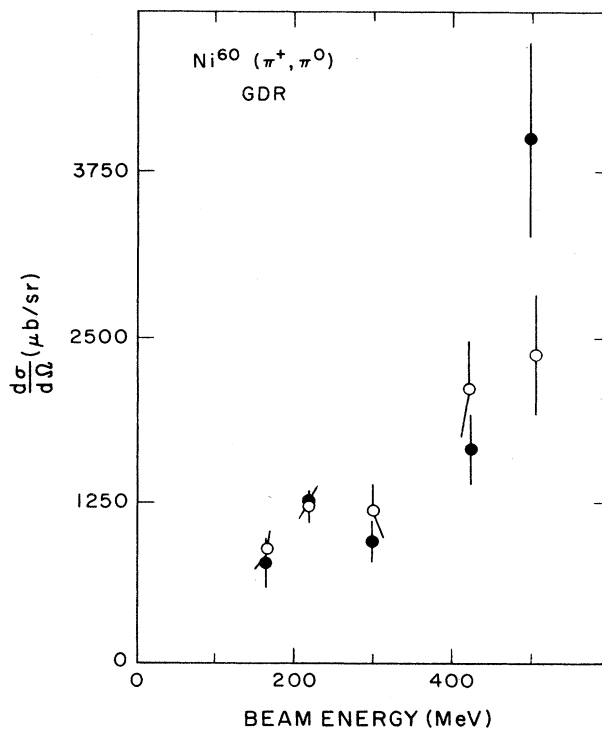


FIG. 4. Peak GDR differential cross sections for pion charge exchange on ⁶⁰Ni are shown as solid points for a range of beam energies, including measurements from Refs. 8 and 9. At higher beam energies this cross section increases sharply, more so than for the IAS peak cross sections shown from Ref. 15 as open points.

matter to pions. For the GDR, this increase in transparency would be sufficient to allow the probing of more central parts of the transition density. This is a more pronounced increase than is seen for the IAS over a similar energy region, but we note that the GDR transition density is more surface peaked than is the IAS transition density.^{1,3} A continued study with more nuclei would be useful to check these results and this hypothesis.

Finally, we note that the increase in the differential cross section for excitation of the GDR at these energies is not accompanied by a similar increase in the background, which scales roughly with the free-nucleon SCX cross section. This cross section is nearly constant in the energy region at which we made these measurements, and is much smaller than near the Δ resonance. It therefore would seem that this high projectile energy is an excellent region in which to determine the characteristics of the GDR.

In summary, we have measured the maximum differential cross section for excitation of the GDR by

SCX at pion energies significantly greater than that for the Δ resonance. These values reflect the increase of nuclear transparency to pions in a way similar to the recently measured values for SCX excitation of the IAS.¹⁵ We also see a large increase in the maximum differential cross section for excitation of the GDR between 425 and 500 MeV. This is a slightly larger increase than that for the IAS differential cross section in the same energy region. This increase, and the relative decrease in the background, make 500 MeV an excellent pion energy at which to conduct future studies of the GDR excited by SCX.

ACKNOWLEDGMENTS

We wish to thank M. J. Leitch, J. L. Ullmann, and J. R. Comfort for assistance in the experiment. This work was supported in part by the U.S. Department of Energy, the National Science Foundation, the U.S.-Israel Bi-National Science Foundation and the Ministry of Immigration and Absorption of the State of Israel.

*Present address: Department of Physics, Harvard University, Cambridge, MA 02138.

†Present address: Physics Department, University of Virginia, Charlottesville, VA 22901.

‡Present address: University of Massachusetts, Amherst, MA 01003.

§Present address: George Washington University, Washington D.C. 20052.

¹N. Auerbach, A. Klein, and Nguyen van Gai, *Phys. Lett.* **106B**, 347 (1981).

²N. Auerbach, *Phys. Rev. Lett.* **49**, 913 (1982).

³N. Auerbach and A. Klein, *Nucl. Phys.* **A395**, 77 (1983); *Phys. Rev. C* **28**, 2075 (1983).

⁴E. Lipparini and S. Stringari, *Phys. Rev. Lett.* **59**, 982 (1987).

⁵H. W. Baer *et al.*, *Phys. Rev. Lett.* **49**, 1376 (1982).

⁶J. D. Bowman *et al.*, *Phys. Rev. Lett.* **50**, 1195 (1983).

⁷A. Erell *et al.*, *Phys. Rev. Lett.* **52**, 2134 (1984).

⁸A. Erell, J. Alster, J. Lichtenstadt, M. A. Moinester, J. D. Bowman, M. D. Cooper, F. Irom, H. S. Matis, E. Piasezky, and U. Sennhauser, *Phys. Rev. C* **34**, 1822 (1986).

⁹F. Irom *et al.*, *Phys. Rev. C* **34**, 2231 (1986).

¹⁰H. W. Baer *et al.*, *Phys. Rev. Lett.* **45**, 982 (1980).

¹¹U. Sennhauser *et al.*, *Phys. Rev. Lett.* **51**, 1324 (1983).

¹²F. Irom, M. J. Leitch, H. W. Baer, J. D. Bowman, M. D. Cooper, B. J. Dropesky, E. Piasezky, and J. N. Knudson, *Phys. Rev. Lett.* **55**, 1862 (1985).

¹³J. L. Ullmann *et al.*, *Phys. Rev. C* **33**, 2092 (1986).

¹⁴F. Irom *et al.*, *Phys. Rev. C* **36**, 1453 (1987).

¹⁵S. H. Rokni *et al.*, *Phys. Lett. B* **202**, 35 (1988).

¹⁶S. Mordechai *et al.*, *Phys. Rev. Lett.* **60**, 408 (1988).

¹⁷A. L. Williams *et al.*, *Phys. Rev. Lett.* **216B**, 11 (1989).

¹⁸H. W. Baer *et al.*, *Nucl. Instrum. Methods* **180**, 445 (1981).

¹⁹R. A. Arndt, Program SAID, Virginia Polytechnic Institute and State University, 1986.

²⁰B. J. Dropesky, G. W. Butler, C. J. Orth, R. A. Williams, M. A. Yates, G. Friedlander, and S. B. Kaufman, *Phys. Rev. C* **20**, 1844 (1979).

²¹W. R. Holley, G. L. Schnurmacher, and A. R. Zingher, *Nucl. Instrum. Methods* **171**, 11 (1980).

²²J. S. Blair, *Lectures in Theoretical Physics*, edited by P. D. Kunz, D. A. Lind, and W. E. Brittin (University of Colorado Press, Denver, 1966), Vol. VIII C, p. 343.

²³D. Ashery, I. Navon, G. Azuelos, H. K. Walter, J. H. Pfeiffer, and F. W. Schlegel, *Phys. Rev. C* **23**, 2173 (1981).

²⁴M. B. Johnson, *Phys. Rev. C* **22**, 192 (1982).